

A EUROPEAN JOURNAL OF CHEMICAL BIOLOGY

CHEM **BIO** CHEM

SYNTHETIC BIOLOGY & BIO-NANOTECHNOLOGY



14/2019

Cover Feature:

U. O. S. Seker et al.

Cellular Biocatalysts Using Synthetic Genetic Circuits
for Prolonged and Durable Enzymatic Activity

A Journal of



WILEY-VCH

www.chembiochem.org



Cellular Biocatalysts Using Synthetic Genetic Circuits for Prolonged and Durable Enzymatic Activity

Recep Erdem Ahan⁺, Behide Saltepe⁺, Onur Apaydin⁺, and Urartu Ozgur Safak Seker^{*[a]}

Cellular biocatalysts hold great promise for the synthesis of difficult to achieve compounds, such as complex active molecules. Whole-cell biocatalysts can be programmed through genetic circuits to be more efficient, but they suffer from low stability. The catalytic activity of whole cells decays under stressful conditions, such as prolonged incubation times or high temperatures. In nature, microbial communities cope with these conditions by forming biofilm structures. In this study, it is shown that the use of biofilm structures can enhance the stability of whole-cell biocatalysts. We employed two different strategies to increase the stability of whole-cell catalysts and decrease their susceptibility to high temperature. In the first

approach, the formation of a biofilm structure is induced by controlling the expression of one of the curli component, CsgA. The alkaline phosphatase (ALP) enzyme was used to monitor the catalytic activity of cells in the biofilm structure. In the second approach, the ALP enzyme was fused to the CsgA curli fiber subunit to utilize the protective properties of the biofilm on enzyme biofilms. Furthermore, an AND logic gate is introduced between the expression of CsgA and ALP by toehold RNA switches and recombinases to enable logical programming of the whole-cell catalyst for biofilm formation and catalytic action with different tools. The study presents viable approaches to engineer a platform for biocatalysis processes.

Introduction

Catalysts can reduce the energy required for any chemical reaction; hence, they are subject to research in various fields. Because various substances, from the production of commodity chemicals to the drugs used in medicine, benefit from catalysis research, the development of efficient and stable catalysts is a highly pursued path.^[1] Regarding cost and eco-friendliness, biological catalysts offer unique advantages over chemical catalysts^[2] because biocatalyzed reactions can be performed under mild conditions with minimized side products and downstream purification costs of the target molecule.^[3]


Pure enzymes obtained from various organisms or the organism itself can be used to catalyze reactions. The use of organisms as catalysts provides efficient and cheap bioprocesses because enzyme purification can be neglected; moreover, the organism can produce and regenerate cofactors required for enzymes.^[4] Owing to advanced tools for genetic manipulations

and metabolic engineering, one can reconstruct multistep biotransformation reactions in different cell machinery, such as *Escherichia coli* and *Saccharomyces cerevisiae*.^[5] A considerable amount of literature shows that, by tweaking existing biological systems, it is possible to produce high-value chemicals, such as opioids,^[6] semisynthetic artemisinin,^[7] vitamin B12,^[8] and indigo dye,^[9] from cheap materials. Nevertheless, biological systems come with shortcomings, such as enzymes can be deactivated easily compared with chemical catalysts and cells cannot tolerate diverse conditions. Moreover, physical conditions in high-yielding industrial processes might not be optimal to support the model of mesophilic organisms.^[10] For instance, the reaction mixing efficiency and solubility of substrate molecules can be improved by increasing the reaction temperature.^[11] Therefore, the usage of thermophilic microorganisms as whole-cell biocatalysts is necessary to obtain higher yields, but optimization of the cell machinery through metabolic engineering, for example; overexpression of genes; or gene knock-out to adjust metabolite fluxes, might not be possible due to a lack of gene manipulating techniques for extremophile organisms.^[12]

Synthetic biology provides options to overcome limitations and opens a way to use mesophilic microorganisms under harsher conditions. One of the solutions provided by synthetic biology is to control and engineer the extracellular matrix (ECM) proteins secreted in biofilms.^[13] Cells can regenerate their enzyme pools in biofilms;^[14] moreover, they can persist under harsh conditions, owing to the unique and self-produced ECM that includes polysaccharides, proteins, and DNA.^[15] Catalytically active biofilms are used in wastewater treatment and xenobiotic remediation, as well as previously in

[a] R. E. Ahan,⁺ B. Saltepe,⁺ O. Apaydin,⁺ Dr. U. O. S. Seker
UNAM-Institute of Materials Science and Nanotechnology
National Nanotechnology Research Center Bilkent University
06800 Ankara (Turkey)
E-mail: urartu@bilkent.edu.tr

[⁺] These authors contributed equally to this work.

 Supporting information and the ORCID identification numbers for the authors of this article can be found under <https://doi.org/10.1002/cbic.201800767>: ALP activity of planktonic cells, plasmid curing analysis and cell viability for planktonic grown cells, SEM images of CsgA-ALP co-expressing cells, SEM images of cells producing csgA for 28 days, biomass quantification by CV staining, plasmid curing analysis and cell viability for biofilm-forming cells, SEM images of CsgA-ALP fusion protein expressing cells, pure ALP protein activity at different temperatures, working principles of the toehold switch, toehold switch controlled GFP expression data, construct maps, and a list of the genetic parts.

vinegar production.^[16] Also, a recent review on engineered bacterial communities has explained the potential of synthetic biology to program biofilm communities for biomanufacturing.^[17]

Curli fibers are the first proteinaceous polymer secreted into extracellular space for use as biofilm matrix scaffolds and can constitute up to 40% of the biovolume of a biofilm.^[18] In a biofilm formed by *E. coli*, fiber expression, secretion, and formation are controlled by the *curli* gene cluster, which consists of seven genes: *csgA*, *B*, *C*, *D*, *E*, *F*, and *G*. It is transcribed from two operons, namely, *csgBAC* and *csgDEFG*. *CsgA* and *CsgB* are the major and minor curli protein subunits, respectively, and they are secreted to the extracellular environment with the help of other curli proteins.^[19] Previous studies have accomplished the engineering of the *CsgA* protein to create biofilms with different functions, such as catalysts,^[20] electrical conductors,^[21] self-assembled materials on solid surfaces,^[22] and adhesives for underwater applications.^[23]

In addition to designing the primary protein sequence of the *CsgA* monomer, to add novel functionalities to biofilm structures, the expression of *CsgA* monomers is vital for initial adherence to the surface and biofilm formation.^[24] Therefore, it is possible to program the ECM of biofilms through tuning and regulating the expression of the *csgA* gene.^[25] In previous studies, researchers built 3D patterned cells as a pressure sensor and low-cost printable cells with a 3D printer by controlling the expression of the *csgA* gene.^[26] Increasing knowledge of RNA biology paves the way for novel elements to tune and control gene expression with complex Boolean logic operations and feedback loops.^[27] For instance, the toehold switch is a de novo designed RNA regulator that acts on the translation process in cells by controlling hairpin formation at the ribosome binding site (RBS) on mRNA. It provides a strategy to engineer multiple switches that are orthogonal to each other to control gene expression from polycistronic mRNA, and result in an almost 300-fold increase in output signal upon induction, relative to the uninduced state, from the test model, while reducing the background signal of the circuit in the nontriggered state.^[28] By using toehold switches, Ebola and Zika virus biosensors were developed;^[29] moreover, in a recent study, researchers used toehold switches for microbial classification.^[30] Aside from RNA regulators, DNA modifying enzymes, such as site-specific serine integrases, are used to build complex logical operations,^[31] to increase the output signals,^[32] and to construct state machines in cells.^[33] In nature, bacteriophages insert their DNA into the bacterial genome by using site-specific integrases through recognition sites called *attB* and *attP*. Because there are serine integrases that irreversibly catalyze the recombination event, it is possible to record information in DNA permanently. Furthermore, serine integrase based genetic circuits demand less metabolic energy than that of other genetic circuits because, following the recombination event, serine integrases are not required for the genetic circuit. Therefore, they are an appealing alternative to RNA switches for constructing genetic circuits.^[34]

In this study, we improved the stability of a model whole-cell catalyst with respect to time and durability at relatively

high temperatures. We used alkaline phosphatase (ALP)-expressing *E. coli* cells as a model to easily monitor the biocatalytic activity through the breakdown of *p*-nitrophenyl phosphate (pNPP) into yellow-colored *p*-nitrophenol (pNP). We used biofilm structures to protect the catalytic activity of whole cells for prolonged times and at a relatively high temperature. In the first strategy, biofilm formation upon overexpression of the *csgA* gene protected catalytically active cells. For the second strategy, we constructed a *CsgA*-ALP fusion protein to protect the enzyme by integrating it into the ECM of the biofilm. The catalytic activity was preserved in both strategies. We further demonstrated that the catalytic activity of biofilms constructed by using both strategies remained unchanged, even at relatively high temperature. Lastly, an AND gate operation was designed and implemented, to program the catalysis function and biofilm formation to prove the robustness of the developed strategy, by using synthetic RNA regulators called toehold switches and recombinases. Based on our results, recombinases performed better than toehold switches under prolonged growth times. Whole-cell biocatalysis can be used to program cells for biomanufacturing. Compared with the cell-free biocatalysis systems, cellular biocatalysts can produce enzymes continuously under optimum reaction conditions. We have demonstrated that utilizing engineered biofilms to improve the stability of biocatalysts is promising; thus, we envision that biofilms, although conventionally considered harmful, can be engineered to accommodate useful functions for industrial applications.

Results and Discussion

Improved stability of whole-cell biocatalysts for prolonged growth

First, we monitored the catalytic activity of planktonic cells for 10 days to test the stability of the cells, which is one of the major concerns of whole-cell biocatalysis. In our whole-cell catalyst model, ALP is expressed in cells and transported to the periplasmic space. Additionally, the substrate, pNPP, is required to diffuse through the outer membrane to interact with ALP enzymes. We observed that suspension cells significantly lost their ability to catalyze the conversion of pNPP to pNP on the 10th day (Figure 1). According to our hypothesis, after a certain time point, suspension cells either lose their plasmid of interest required for ALP production or become unviable for the production of ALP as they start to die. Therefore, plasmid curing and cell viability were examined after 3, 6, and 10 days. We observed that cells maintained the plasmid of interest for ALP production for 10 days, but the viable cell number decreased over prolonged growth (Figure S1 in the Supporting Information). Thus, the preservation of cell viability is a critical point for engineering more stable whole-cell catalysts.

To overcome this issue, we used the biofilm-forming ability of *E. coli*. Also, for strict control of biofilm formation, *E. coli* MG1655 $\Delta csgA$ cells were used. We employed two strategies to prolong the catalysis activity of the enzymes produced by cells. In the first strategy, we induced biofilm formation by

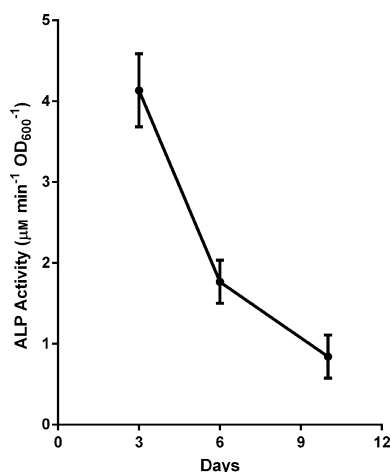


Figure 1. ALP activity of cells grown in planktonic phase for 10 days. The ALP activity was measured for 3, 6, and 10 days. pNPP substrate conversion [μM] over time by the ALP enzyme was normalized to cell density. All experiments were performed in triplicate.

overexpressing the major curli subunit, CsgA (Figure 2A). Through this strategy, we aimed to protect cells from stress caused by increased growth periods. In the second strategy, the ALP enzyme is fused with CsgA protein (Figure 2B). The CsgA-ALP fusion proteins are secreted to the extracellular space following translation and form a synthetic network of fibers with embedded ECM in the biofilms. The strategy aimed to increase the stability of the ALP enzymes by protecting them from intracellular proteases and extracellular factors, such as potential inhibitors or physical stressors. Also, the substrates can be readily accessible to enzymes without encountering any diffusion barrier.

To assess the effect of ALP fusion on CsgA fibers, we examined cells producing only CsgA and CsgA-ALP fusion proteins by means of SEM and TEM. Following induction, we observed that both types of cells produced an excellent network of curli fibers to form clusters covering themselves (Figure 2C, D). On the other hand, we observed that the overexpression of ALP had no observable effect on curli fibers in the case of CsgA and ALP coexpression (Figure S2).

Furthermore, to validate that both the ALP-CsgA coexpressed system and ALP-CsgA fusion networks were able to breakdown the pNPP substrate, we conducted a phosphatase assay to monitor pNPP conversion by ALP. Results showed that both systems were finely controlled by inducers over 3 days and were able to convert pNPP into pNP in the curli network in both systems (Figure 2E, F).

The CsgA curli subunit was induced and grown for 28 days in culture plates to test the protective effect of biofilm formation on whole-cell biocatalyst activity with prolonged growths. Growth medium for the cells was renewed every 3 days to support continuous biofilm formation. SEM results showed that different incubation times led to similar curli network formation (Figure S3). Also, biomass formation at different time points over 28 days was quantified by means of crystal violet (CV) staining. We observed a significant amount of steady biomass accumulation after washing adhered cells to remove

loosely bound cells (Figure S4). We induced the cells for ALP expression as stated in Figure 3 to measure the catalytic activity of cells in the biofilm. Before induction, biofilms were washed to remove planktonic cells that did not adhere to the surface. Results showed that the biofilm structure was able to preserve the catalytic activity of cells for at least 21 days. We observed maximum whole-cell enzymatic activity at day 9 (Figure 3A). The total catalytic activity of cells in the biofilm increased for 9 days then decreased for subsequent days. The cells in the curli network were even able to express the ALP enzyme on day 21, whereas, as previously mentioned, planktonic cells lost their ability to express proteins due to a decrease in viability. Therefore, we also checked the viability of CsgA expressing cells grown for 3, 9, and 28 days. The cell viability increased after 28 days compared with growth for 3 and 9 days (Figure S5B). Previous reports stated that curli subunit overexpression enabled cells to attach to the surface and promote biofilm formation.^[24,35] Biofilm formation is a universal strategy for many bacteria to survive in nutrient-limiting conditions and in a high concentration of toxic molecules.^[36] The medium conditions for prolonged growth can be problematic due to the nutrition depletion and the accumulation of toxic materials. Therefore, the increase in survivability for extended times can be explained through biofilm formation.

On the 28th day, we observed that ALP enzymes produced by cells were not functional for the conversion of pNPP into pNP. We hypothesized that cells lost their plasmid-containing ALP expressing genes because antibiotic selection pressure on cells in the biofilm might not be as effective as previously because the biofilm also provides resistance to antibiotics.^[37] Therefore, plasmid curing was monitored for 3 and 28 days. At these time points, plasmid isolation was performed on the cells, and digested with a single restriction enzyme. The corresponding bands for single-cut ALP expression plasmid were observed for all day time points (Figure S5A). A significant decrease in whole-cell activity on the 28th day cannot be explained by either plasmid loss or decreased cell viability. Although there is room to improve the system further, in-depth analysis of cellular metabolism in the biofilm is required, especially in the context of gene regulation, to understand the governing reasons for activity loss. However, our results suggest that biofilm formation preserves whole-cell catalytic activity significantly longer than that of conventional suspension cultures.

Next, we investigated whether curli could protect the ALP enzymes if they were fused to the CsgA protein. The curli fiber network is resistant to many denaturing agents and embedded in the biofilm, along with other ECM polymers.^[38] The CsgA-ALP fusion system aims to utilize these preservative effects of biofilm formation for the enzyme itself. We hypothesized that other biopolymers present in the biofilm ECM, such as DNA and polysaccharides, could protect the ALP enzyme upon immobilization onto CsgA fibers. To prove this hypothesis, ALP enzymes were fused to the C terminus of the CsgA protein. Also, we added a tandem repeat of GGGGS flexible linker to minimize the interaction of ALP and CsgA proteins. Cells harboring the expression plasmid were induced to produce CsgA-

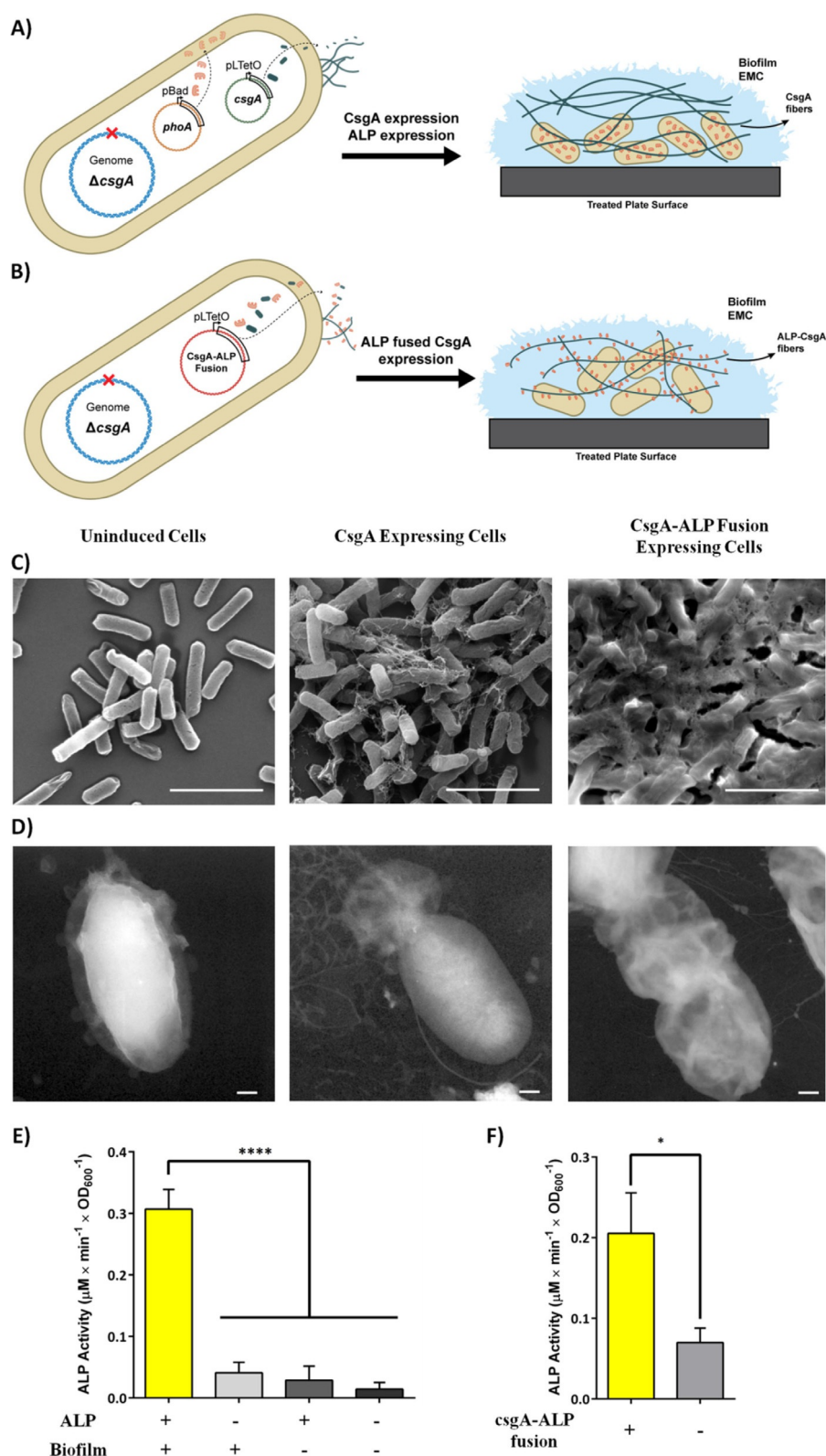


Figure 2. A) Representation of the CsgA and ALP coexpression system. CsgA expression was controlled by pLTetO-inducible promoter, whereas the pBad-inducible promoter was used for ALP expression. B) The CsgA-ALP fusion system. We expressed ALP as a fusion partner with the CsgA curli subunit under the control of a pLTetO promoter. C) SEM and D) TEM images of uninduced cells, CsgA-ALP fusion protein expressing cells, and native CsgA cells. Scale bars: 1 μm (SEM images) and 200 nm (TEM images). E) ALP activity of whole cells after curli network formation for 3 days. Biofilm+ cells were induced with anhydrotetracycline (aTc) for both control and positive samples. ALP+ cells were induced with 0.2% arabinose for both control and positive samples. Biofilm- and ALP- samples had no inducer, but were instead treated with inducer solvents (final concentration of 0.05% ethanol for aTc; water for arabinose). F) ALP activity of the CsgA-ALP fusion fiber producing cells after forming a curli network for 3 days. For the results shown in E) and F), experiments were performed in triplicate. One-way ANOVA (E) and Student's t tests (F) were applied for significance analysis (* $p < 0.05$, ** $p < 0.001$).

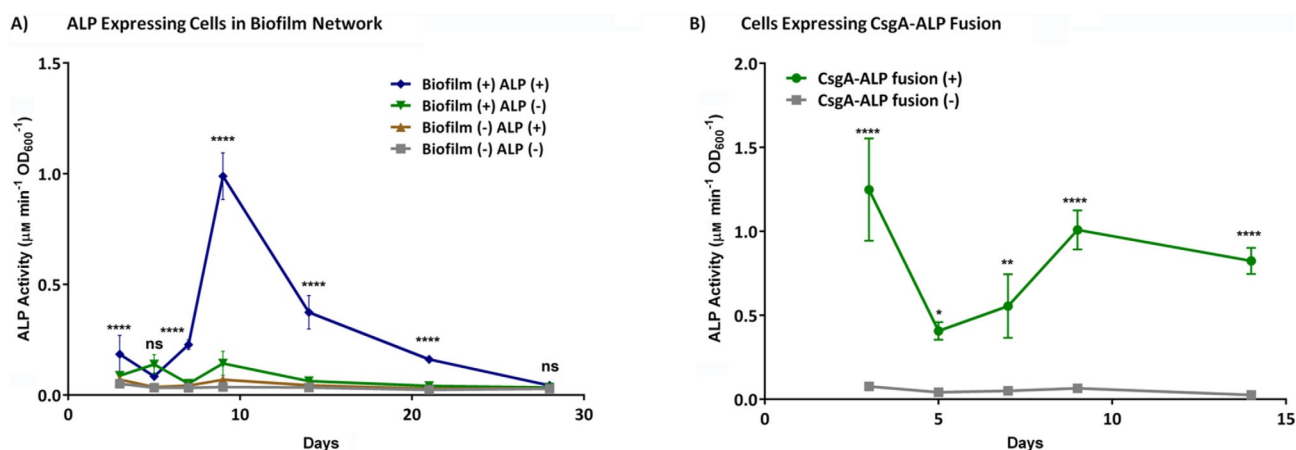


Figure 3. ALP activity of A) CsgA-ALP coexpressed cells and B) cells expressing CsgA-ALP fusion protein. Coexpression samples and fusion expressing samples were allowed to form biofilms for 28 and 14 days, respectively, during which time their enzymatic activity was measured at the time points noted on the graphs. On the day of measurement (3, 5, 7, 9, 14, 21, and 28 days), we stopped biofilm formation for cells coexpressing CsgA and ALP, and ALP expression was induced with arabinose. Biofilm+ cells were induced with aTc for both control (-) and positive (+) samples. ALP+ samples were induced with arabinose for both control (-) and positive (+) samples. Biofilm- and ALP- samples were not induced with the respective inducers, but instead treated with inducer solvents (final concentration of 0.05% ethanol for aTc; water for arabinose). For the fusion protein expressing cells, they were either treated with aTc or not. Following induction, ALP activities were determined through the phosphatase assay. Student's t tests were performed to determine the significance (** $p < 0.001$, **** $p \leq 0.0001$; ns: no significance).

ALP fusion protein for 14 days. Monitoring the enzyme activity for 14 days was chosen because the whole-cell catalytic activity of the system in the first strategy significantly declined after 14 days. Following induction, we observed that cells obtained after 3, 5, 7, 9, and 14 days were able to produce curli fibers coupled with ALP enzymes; however, fibers showed slightly different structures than that of the native curli fibers (Figure S6).

In terms of the catalytic activity, the CsgA-ALP fibers were able to hydrolyze pNPP substrates without a decrease on the 14th day (Figure 3B). Because continuous expression and secretion of the CsgA-ALP fusion protein resulted in fiber formation in the ECM of the biofilm, any metabolic changes in cell metabolism in the context of gene regulation would not affect the total catalytic activity of the biofilm. Therefore, this system could be a valid solution for the loss of activity observed in our previous strategy.

Resistance to high temperature provided by biofilms

We investigated the preservative capabilities of biofilms on whole-cell catalysis to a broader extent. High temperature was chosen as a stressor. Systems resistant to high temperature were assessed by using the same experimental model with heat treatment for a relatively long time. Pure ALP enzyme was incubated to find reasonable conditions at various temperatures for different times. A temperature of 75 °C for 2 h had a deleterious effect on the activity of pure ALP enzyme, whereas 55 °C had no effect (Figure S7). Both systems, either cells expressing ALP and CsgA proteins or CsgA-ALP fusion protein, were induced to form biofilms for 9 days then treated at 75 °C for 2 h. Following heat treatment, whole-cell ALP activity was measured by means of the phosphatase assay, and activity changes were calculated relative to untreated cells. Cells ex-

pressing curli fibers and ALP enzyme separately retained their whole-cell ALP activity almost entirely upon 2 h of heat treatment at 75 °C (Figure 4A). This was also valid for the fusion protein expressing cells, whereas the ALP activity of planktonic cells dropped by almost 50% following the same heat treatment (Figure 4A). These results indicated that biofilm formation not only preserved the catalytic activity for prolonged growth, but also under a relatively high temperature, compared with the optimum growth temperature of the model organism.

Furthermore, we examined fibers by means of SEM after heat treatment. The results showed that CsgA fibers were still visible under SEM after heat treatment and there was no noticeable effect of heat on the fibers or cells themselves (Figure 4B). In support of our observations, previous reports state that CsgA fibers are heat resistant due to their amyloid characteristics.^[39]

AND gate operation with toehold switches and recombinases

After showing the preservative effects of biofilm formation on biocatalysis, we next sought to integrate synthetic logic gates to increase the robustness of our system and provide a means to fine-tune our systems. For this purpose, a newly engineered riboregulator-based switch system, namely, a toehold switch, was employed. These switches mostly regulate the system between transcription and translation. The toehold switch system is composed of two regulatory RNA sequences: switch and trigger. Switch RNA forms a hairpin structure after transcription of the gene of interest blocking the translation machinery. However, in the presence of trigger RNA, this hairpin structure is disturbed to make the RBS accessible, so that the ribosome initiates the translation machinery (Figure S8). This has been

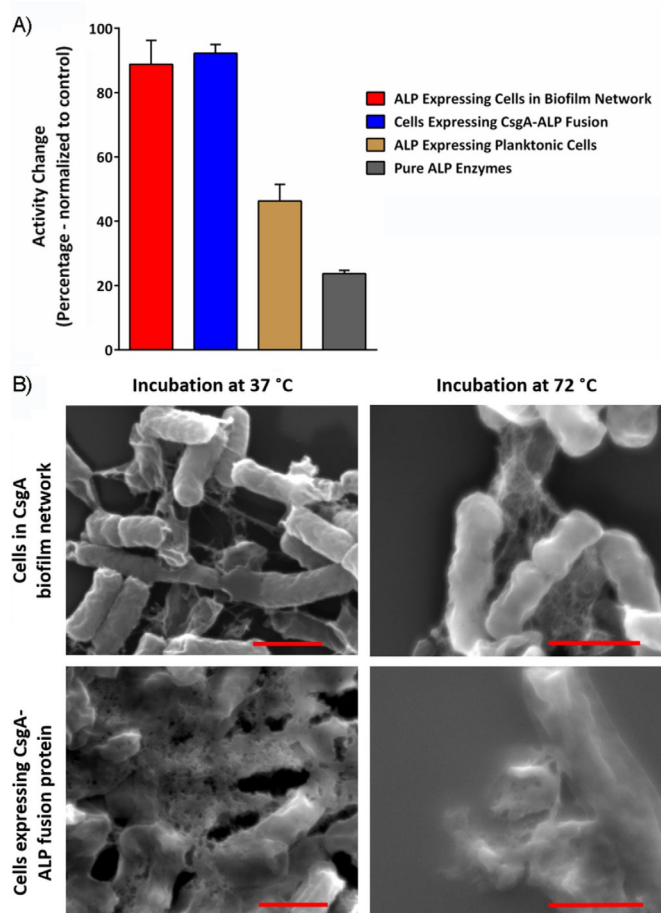


Figure 4. A) Enzymatic activity changes to CsgA and ALP coexpressing cells and CsgA-ALP fusion protein expressing cells upon heat treatment at 75 °C for 2 h compared with suspension cell culture and pure ALP enzyme under the same conditions. Each group was normalized to its control group (incubated at 37 °C for 2 h). B) SEM images of both CsgA and ALP coexpressing cells and CsgA-ALP fusion expressing cells before and after heat treatment. Scale bars: 1 μm.

shown to provide tight control over the implemented system. We first tried to replicate the results of the toehold switch with green fluorescent protein (GFP) in BL21(DE3) host cells to test its effect upon induction, as reported previously by Green et al.^[28] It was observed that implementing toehold switch in a basic GFP reporter inducible circuit provided almost 50-fold increase upon induction (Figure S9).

To control CsgA and ALP expression with the toehold switch mechanism, Switch1 and Switch2 sequences were introduced upstream of the *csgA* and *phoA* genes, respectively. The switch regulated genes were constitutively transcribed on the same polycistronic mRNA with truncated proD promoter. Transcription of the trigger sequences (Trigger1 for CsgA and Trigger2 for ALP) was controlled with aTc and arabinose inducible systems to initiate CsgA and ALP translation, respectively. This system works as an AND gate that shows enzymatic activity only in the presence of both inducers; otherwise, no action is observed (Figure 5A).

We proceeded to test the AND operation in our systems. Cells were induced with aTc for translation of the *csgA* gene

for 5 days, and *phoA* translation was subsequently switched on with arabinose. An induction period of 5 days was chosen to give ample time for bacteria to form the curli network and biofilm. CsgA fibers were visible under SEM after 5 days of induction (Figure 5B). The total catalytic activity of cells that co-produced ALP and CsgA proteins was significantly higher than that of the uninduced states, but we observed similar total catalytic activities for aTc and only arabinose induced cells (Figure 5C). The results indicate that, despite the toehold switches being unique regulatory elements to control protein production in suspension culture, their performance in biofilm forming cells make them unfavorable for building logic gates due to high leakiness. The cell densities at each point and correlation between enzyme concentration and measured activity are provided in Figures S19, S20, and S21. The cell densities were used to normalize the measured activities for the ALP enzyme.

After evaluation of the toehold switch integrated AND gate, we reconstituted the AND logic gate with a new strategy to provide tighter control and to overcome the leakage issue over time. Hence, a recombinase-based AND logic gate was constructed (Figure 5A). In the modified circuit, both CsgA and ALP expression were controlled with an inverted proD promoter located between anti-aligned attB/attP sites. The genes can only be transcribed after expression of the corresponding recombinase. The inverted proD promoter between Bxb1 attB/attP sites was placed upstream of the *csgA* gene, whereas TP901 attB/attP sites were used for the inverted promoter located upstream of the *phoA* gene.

Expression of Bxb1 recombinase was under control of the pLtetO promoter, whereas TP901 recombinase expression was controlled with the pLlacO promoter. Cells were induced to produce Bxb1 recombinase for 1 day, then growth medium (M63 minimal medium supplemented with proper antibiotics, 0.2% glucose (w/v), and 1 mM MgSO₄) was renewed to remove the inducer to stop unnecessary expression of Bxb1 recombinase. We grew the cells for 2 days in the restored medium for CsgA expression and biofilm formation. CsgA fiber formation was examined under SEM following growth. The induced cells formed visible fibers, whereas we did not observe any fibers in the uninduced sample (Figure 5D). Following CsgA expression, we washed the biofilms with doubly distilled (dd) H₂O to remove planktonic cells. TP901 recombinase was induced for 1 day to express the ALP enzyme. After induction, the total catalytic activity of the biofilm was measured by means of the phosphatase assay. Although the highest activity was obtained from cells induced with both inducers, we also observed that uninduced cells, as well as only CsgA expressing cells, had slightly active pNPP breakdown. However, only ALP expressing cells had negligible activity (Figure 5E). Results indicate that, although leakiness is a cross-cutting issue for the recombinase, similar to toehold switches in logic gate design for increased growth periods, recombinase performance was better than that of the toehold switches. All in all, on the contrary to the toehold-integrated system, recombinase-based circuits provide the opportunity for tighter control over prolonged growth times required for biofilm formation.

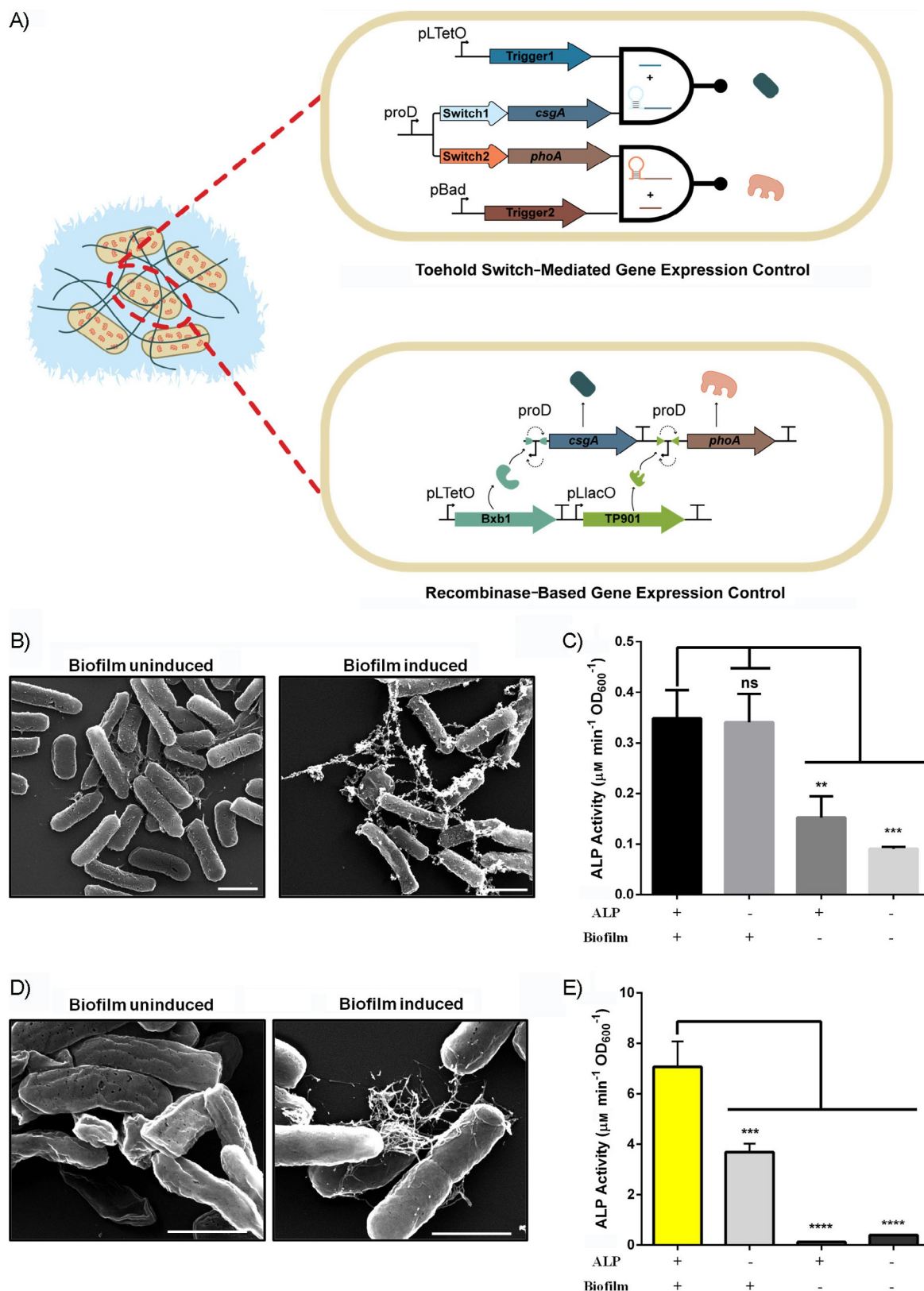


Figure 5. A) Representation of the toehold switch integrated system (top) in which the curli protein and ALP were expressed separately upon induction with aTc and arabinose, respectively, and the recombinase-based expression system (bottom), in which the curli protein and ALP were expressed individually upon induction of Bxb1 and TP901, respectively. B) SEM images of uninduced and induced toehold integrated systems after 5 days of biofilm formation. Scale bars: 1 μm . C) Enzymatic activity of the toehold integrated system after 5 days of biofilm formation. One-way ANOVA was performed for significance analysis ($*p \leq 0.05$). D) SEM images of the uninduced and induced recombinase-based expression system following 1 day of induction and 2 days of inducer-free growth. Scale bars: 1 μm . E) Enzymatic activity of the recombinase-based expression system. One-way ANOVA was performed for significance analysis ($****p \leq 0.0001$).

Conclusion

This study showed that engineering of biocatalysis processes is a viable way to overcome issues such as stability. Synthetic cellular systems utilizing biofilms preserve enzymatic activity over a longer period of time than that of regular biocatalysis systems and are protected from harsh conditions, such as high temperature. Bacterial whole-cell catalysts are promising candidates for engineering cascaded enzymatic reactions. They can be programmed to carry out multiple tasks, as discussed herein. However, there is much scope to improve the way we engineer cells to accomplish numerous tasks in conjugation with their enzymatic activities.

We followed two different strategies in our whole-cell biocatalyst design. The catalytic activity of whole cells is preserved in both strategies over extended growth times and at high temperatures. Biofilms can be engineered as biocatalysts by either functionalization of CsgA fibers or intracellular expression of the enzyme of interest along with extracellular expression of CsgA. Although we used a model enzyme (ALP) to show that two different strategies were valid for increasing the catalytic stability of whole-cell biocatalysts, these approaches could be exploited for different enzymes. The demand from each enzyme for the continuous supply of cofactors, ATP, vitamins, and indiffusible substrates (xenobiotics or large polysaccharides) may differ. The enzymes that requires cofactors can be expressed intracellularly, as shown in the first approach; on the other hand, the enzymes can be secreted to the extracellular space to process membrane-indiffusible substrates, as shown in the second approach.

Synthetic biology offers many possibilities for this purpose: by employing genetic logic gates or recording systems, whole-cell catalysts can be programmed to sense-react with target molecules. In our design, we built a simple AND gate with dual functionality. The AND gate can operate only in the presence of defined chemicals. This proof-of-concept study provides a path for designing improved whole-cell biocatalysts that can sense the presence of a target substrate, transport the target molecule inside the cell, or secrete necessary enzymes into the extracellular environment. Such a system can only rely on strong synthetic genetic regulation, which can preserve the cellular economy regarding energy. Additionally, synthetic circuits can be programmed to remove the toxicity of substrates on the enzymes by metabolizing the substrates for other activities.

In summary, we designed a biodevice that could sense the presence of target molecules and activate biofilm formation and enzymatic activity within cells. Biofilm structures are perfect biomaterial systems because they can provide long-term stability for the synthesized enzymes. We followed two approaches: biofilm protein-ALP coexpression or the formation of ALP-fused biofilm structures. Both of these approaches were successful at preserving enzyme activity against the detrimental effects of elevated temperatures. Herein, we propose that the biofilm architecture is a living factory that can stick on surfaces without any need for surface modification and preserves the enzyme activity. We believe that genetically fused enzyme-

biofilm structures, along with synthetic biology based logic gate operations, are promising innovative solutions for industrial settings as well.

Experimental Section

Cell strains, growth and medium conditions, and transformations: The *E. coli* MG1655 strain with an ompR234 mutation, to enhance curli expression, and with a proexpression cassette, to use the aTc-inducible pLtetO promoter, was used as a host cell for the expression of all proteins. Toehold switch calibration experiments were conducted with the *E. coli* BL21 DE3 strain then changed to the MG1655 strain. Growth was started in lysogeny broth (LB; 10 g tryptone, 5 g yeast extract, 5 g NaCl) and the medium was changed to M63 minimal medium (VWR) for experiments, unless otherwise stated. Transformations of constructs into host cells were performed with chemically prepared competent cells of host strains.

Cloning of constructs: All cloning experiments were performed in accordance with the Gibson assembly method.^[41] Genes were amplified from the genome or other constructs with primers designed for Gibson assembly by means of a polymerase chain reaction (PCR), adding overhangs to the 5'- and 3'-ends of the PCR product overlapping with backbones. We performed all PCR reactions with Q5 HF polymerase (New England Biolabs), and all restriction digestion reactions were performed with appropriate restriction endonucleases (New England Biolabs), according to the manufacturer's instructions. All constructed plasmid vector maps used herein are shown in the Supporting Information (Figures S10–S18). We verified each insert through Sanger sequencing (GeneWiz, Inc., South Plainfield, NJ, USA). All genetic parts used in this study are listed in the Supporting Information (Table S1).

aTc-inducible CsgA construct (Figure S10): The *csgA* gene from the *E. coli* genome was cloned into the pZ vector (p15 origin of replication with chloramphenicol resistance gene (cmR)) under control of the pLtetO promoter.

Arabinose-inducible ALP construct (Figure S11): The *phoA* gene from the *E. coli* genome was cloned into the pBAD/His-B plasmid backbone^[40] (Addgene #31909, a gift from Vladislav Verkhusha (Albert Einstein College of Medicine); pBR322 origin of replication with ampicillin resistance gene (ampR)) under the control of AraC promoter.

Fusion construct (Figure S12): Fusion of *csgA* and *all* genes were made by cloning of both genes into the pZ vector under control of a pLtetO promoter with a His₆ tag at the 3'-end.

Toehold switch (Figures S13 and S14): Toehold switch integrated GFP for calibration was cloned under control of the T7 promoter in pZ backbone cmR, whereas Trigger1 was cloned in the pet22b backbone (ampR) under control of the T7 promoter.

Toehold-controlled CsgA and ALP (Figures S15 and S16): Integration of toehold parts into *csgA* and *rhoA* genes was performed by cloning of the *csgA* gene with Switch1 and the *phoA* gene with Switch2 sequences into the pZ backbone (cmR) under control of the proD promoter in a bicistronic manner, whereas Trigger1 and Trigger2 were cloned under control of pLtetO and pBAD promoters into the pBAD/His-B backbone (ampR), respectively.

Recombinase-controlled CsgA and ALP expression construct (Figure S17): The dual recombinase-controlled plasmid was constructed by cloning the *csgA* and *phoA* genes downstream of in-

verted proD promoters between anti-aligned attB and attP sites of Bxb1 and TP901 recombinases. The fragments that contained the reversed proD promoter with attB and attP sites were synthesized by GeneWiz Inc.

Recombinase expression vector for CsgA and ALP expression construct (Figure S18): The AraC/pBAD promoter that controlled the expression of TP901 in the dual recombinase-controller plasmid^[41] (Addgene #44456 a gift from Drew Endy) was changed with pLacO promoter.

Biofilm network formation and enzyme induction

For planktonic cells: Cells were grown in LB medium at 37 °C, 180 rpm, overnight; diluted 1:100 into fresh LB on the experiment day; and grown at 37 °C and 180 rpm until the OD₆₀₀ reached 0.6. Then, cells were collected at 1000g for 10 min and resuspended in M63 minimal medium supplemented with 0.2% glucose (*w/v*), 1 mM MgSO₄, and appropriate antibiotics. Resuspended cells (2 mL) were transferred into wells of 24-well cell culture treated plates (Corning) at 30 °C for 3 to 10 days, depending on the duration of the experiment. Afterward, we renewed old media every 3 days by discarding the old medium and adding the new medium without washing. On the corresponding experiment day, cells were collected at 1000g for 10 min and resuspended in fresh M63 minimal medium with previously specified supplements. For ALP production, cells were induced with 0.2% arabinose (*w/v*) and incubated at 37 °C for 4 h. We collected cells (1000g for 10 min) to measure ALP activity at the end of incubation and the phosphatase assay was performed.

For CsgA and ALP coexpression: All cells were grown in LB medium at 37 °C, 180 rpm, overnight; diluted 1:100 into fresh LB on the experiment day; and grown at 37 °C, 180 rpm, until the OD₆₀₀ reached 0.6. Then, cells were collected at 1000g for 10 min and resuspended in M63 minimal medium supplemented with 0.2% glucose (*w/v*), 1 mM MgSO₄, and appropriate antibiotics. Curli formation was induced with 250 ng μL⁻¹ aTc, unless otherwise stated. Resuspended cells (2 mL) were transferred into wells of 24-well cell culture treated plates (Corning) to form a curli network at 30 °C for 3 to 28 days, depending on the duration of the experiment. Old media were renewed every 3 days by discarding the old medium and adding the new medium without washing. On the corresponding experiment day, which was the end of curli formation, media were discarded, and biofilms at the bottom of each well were washed four times with distilled water to remove the planktonic cells. Before the phosphatase assay, ALP was induced with 0.2% arabinose (*w/v*) and incubated at 37 °C for 4 h. At the end of ALP induction, media were discarded and the phosphatase assay was performed.

For CsgA-ALP fusion: All cells were grown in LB medium at 37 °C, 180 rpm, overnight; diluted 1:100 into fresh LB on the experiment day; and grown at 37 °C, 180 rpm, until the OD₆₀₀ reached 0.6. Then, cells were collected at 1000g for 10 min and resuspended in M63 minimal medium supplemented with 0.2% glucose (*w/v*), 1 mM MgSO₄, and appropriate antibiotics. Curli formation was induced with 250 ng μL⁻¹ aTc, unless otherwise stated. Resuspended cells (2 mL) were transferred into wells of 24-well cell culture treated plates (Corning) to form a curli network at 30 °C for 3 to 14 days, depending on the duration of the experiment. Old media were renewed every 3 days without washing. On the corresponding experiment day, which was the end of induction for biofilm formation, media were discarded, and biofilms at the bottom of wells were washed four times with distilled water to remove the plank-

tonic cells before the ALP activity was measured with the phosphatase assay.

For toehold switches: All cells were grown in LB medium at 37 °C, 180 rpm, overnight; diluted 1:100 into fresh LB on the experiment day; and grown at 37 °C, 180 rpm, until the OD₆₀₀ reached 0.6. Then, cells were collected at 1000g for 10 min and resuspended in M63 minimal medium supplemented with 0.2% glucose (*w/v*), 1 mM MgSO₄, and appropriate antibiotics. Curli formation was induced with 250 ng μL⁻¹ aTc, unless otherwise stated. Resuspended cells (2 mL) were transferred into wells of 24-well cell culture treated plates (Corning) to form a curli network at 30 °C for 5 days. We renewed the old media every 3 days. On the corresponding experiment day, which was the end of curli formation, media were discarded, and adhered cells at the bottom of each well were washed four times with distilled water. Before the phosphatase assay was performed, ALP was induced with 0.2% arabinose (*w/v*) and incubated at 37 °C for 4 h. At the end of ALP induction, media were discarded, and the phosphatase assay was performed.

For recombinase-based expression: All cells were grown in LB medium at 37 °C, 180 rpm, overnight; diluted 1:100 into fresh LB on the experiment day; and grown at 37 °C, 180 rpm, until the OD₆₀₀ reached 0.6. Then, cells were collected at 1000g for 10 min and resuspended in M63 minimal medium supplemented with 0.2% glucose (*w/v*), 1 mM MgSO₄, and appropriate antibiotics. Curli formation was induced with 250 ng μL⁻¹ aTc, unless otherwise stated. Resuspended cells (2 mL) were transferred into wells of 24-well cell culture treated plates (Corning) to form a curli network at 30 °C for 18 h. At the end of curli formation, media were renewed, and cells were incubated for 24 h before ALP production. At the end of incubation, ALP was induced with isopropyl-β-D-thiogalactopyranoside (IPTG; 1 mM) and incubated at 30 °C for 18 h. At the end of ALP induction, media were renewed, and cells were incubated for 24 h before the phosphatase assay was performed.

High-temperature experiments: One unit of purified ALP enzyme (made in the lab) was incubated at 55 °C for 30, 60, 120, and 240 min; at 75 °C for 15, 30, 60, and 120 min; and at 95 °C for 5, 15, 30, and 60 min. Following incubation, the activity of ALP enzymes was determined from the phosphatase assay for all conditions.

For both coexpressed and fusion samples, biofilm network formation was induced for 9 days following ALP enzyme induction was performed, as stated previously. Afterward, samples were heated at 75 °C for 2 h. For planktonic cells, ALP was induced at 37 °C for 4 h; then, cells were incubated at 75 °C for 2 h. Pure enzymes were directly incubated at 75 °C for 2 h without any pretreatment. After heat treatment, ALP activity was measured with the phosphatase assay, and the activity change was calculated. We normalized each group to its untreated control, which was incubated at 37 °C for 2 h.

ALP enzymatic activity measurements through the phosphatase assay and data analysis: Enzymatic activity of planktonic cells was measured by resuspending cells in substrate solution (200 μL; 1 mM MgCl₂, 1 mM ZnCl₂, 0.1 M glycine, pH 10.4) with and without pNPP substrate (0.5 mM). The absorbance at λ = 600 and 405 nm was measured continuously for 2 h at 37 °C for all samples in the 96-well plate. To normalize the phosphatase activity, the background signal at λ = 405 nm (absorption of cells suspended in reaction buffer without pNPP) was subtracted from the reaction (absorption of cells suspended in reaction buffer with pNPP) signal at saturation point. Then, the obtained value was divided by the total amount of times that passed before saturation, and the OD₆₀₀ of cells suspended in substrate solution without pNPP.

For biofilm samples, substrate solution (400 μL) with and without 0.5 mM pNPP substrate was added to biofilm samples formed at the bottom of the 24-well plate. Same as described above, all samples were measured continuously at $\lambda=405$ nm for 2 h at 37 °C. The obtained value was divided by the total amount of times that passed before saturation, and the OD_{600} of cells suspended in substrate solution without pNPP.

All measurements were performed on a microplate reader (Molecular Devices, M5 Spectramax). We performed at least three biological replicates for each experiment and normalized data to both cell density and time was used for experimental analysis.

GFP reporter circuit activity measurement: The toehold integrated GFP expression system was composed of two constructs, in which one contained a switch sequence integrated *gfp* gene under control of a T7 promoter. Another contained the trigger part under control of a T7 promoter. Cells containing both constructs and a control group with no trigger construct were grown overnight and diluted 1:100 in fresh LB medium supplemented with appropriate antibiotics. Then cells were grown until the OD_{600} reached 0.6 and induced with IPTG (1 mM) for 3 h at 37 °C, 180 rpm. Then GFP signal was measured under excitation at $\lambda=485$ nm and emission at $\lambda=538$ nm. All measurements were conducted with at least three biological replicates and normalized to cell density.

SEM and TEM sample preparation and operation: For SEM sample preparation, each sample was dropped onto a silicon wafer. Cells were fixed with 2.5% glutaraldehyde dissolved in 1 \times PBS at 4 °C, overnight. Afterward, all wafers were washed twice with 1 \times PBS; twice with ddH_2O ; and once with 25, 50, and 75% EtOH, for 5 min each. The last washing step with 100% EtOH was repeated three times for 10 min each. Then samples were dried with a critical point drier (CPD) and mounted on stubs for SEM imaging. The stubs were coated 8 nm thick with Au/Pd alloy. The cells were visualized under an environmental scanning electron microscope (Tecnia).

For TEM samples, the bottom of each well for each sample was scraped and collected into a 1.5 mL microfuge tubes with 1 \times PBS solution. A drop (20 μL) from collected samples was put onto a carbon-coated grid and incubated for 1 min. The excess amount of samples were washed three times with distilled water for 1 min. Furthermore, samples were counterstained with a drop (20 μL) of 2% (*w/v*) uranyl acetate for 20 s. The excess amount of fluid was removed from the grid before visualization with TEM (FEI Tecna).

CV staining: CsgA and ALP coexpressed cells, only ALP expressed cells, and empty cells were used to quantify biomass formation up to 28 days. For CV staining, the medium from each sample in the 24-well plates was discarded. Remaining biofilm was washed with ddH_2O four times. Following washing, cells were stained with 0.2% (*w/v*) CV (400 μL ; Sigma). After 10 min of incubation at room temperature, each well was rewashed at least four times with ddH_2O . Images for biomass quantification were recorded by using the ChemiDoc MP imaging system (BioRad).

Cell viability assay: For cell viability assessment over time, planktonic cells and CsgA and ALP coexpressed cells were grown in 24-well plates, as stated previously. At the specified time points, each sample (100 μL) was collected and serial dilution was performed up to 10^6 . For biofilm samples, the planktonic cells were removed by washing prior to sampling. Each sample (100 μL) from the final dilution factor was inoculated in Agar plates supplemented with appropriate antibiotics and grown overnight at 37 °C. Colony-form-

ing units (CFUs) were calculated for all samples. We performed all of the experiments with at least three biological replicates.

Plasmid curing assay: For plasmid curing assessment over time, planktonic cells and CsgA and ALP coexpressed cells were grown in 24-well plates, as stated previously. At the specified time points, cells were collected and plasmids were isolated with GeneJET Plasmid Miniprep Kit (Thermo Scientific), according to the manufacturer's instructions. After plasmid DNA isolation and quantification with a NanoDrop 2000 spectrophotometer (Thermo Scientific), all samples were digested with KpnI enzyme (New England Biolabs), according to the manufacturer's instructions and visualized with the ChemiDoc MP imaging system (BioRad).

Statistical analysis: All data were expressed as mean \pm standard error of the mean. One-way ANOVA was used to determine the significance in Figures 2E and 5B,E. The Student's *t* test was used to check the significance in Figures 2F and 3 (GraphPad Prism v6).

Acknowledgements

This study was supported by TUBITAK (grant no. 114M163). U.O.S.S. expresses his thanks for a TUBA-GEIP award. We thank Elif Duman for technical help.

Conflict of Interest

The authors declare no conflict of interest.

Keywords: biofilms • curli fibers • enzymes • synthetic biology • whole-cell biocatalysis

- [1] K. Cao, J. M. Cai, X. Liu, R. Chen, *J. Vac. Sci. Technol. A* **2018**, *36*, 010801.
- [2] B. Lin, Y. Tao, *Microb. Cell Fact.* **2017**, *16*, 106.
- [3] C. C. de Carvalho, *Microb. Biotechnol.* **2017**, *10*, 250–263.
- [4] J. Wachtmeister, D. Rother, *Curr. Opin. Biotechnol.* **2016**, *42*, 169–177.
- [5] a) C. P. Badenhorst, U. T. Bornscheuer, *Trends Biochem. Sci.* **2018**, *43*, 180–198; b) V. G. Yadav, M. De Mey, C. G. Lim, P. K. Ajikumar, G. Stephanopoulos, *Metab. Eng.* **2012**, *14*, 233–241; c) J. Nielsen, J. D. Keasling, *Nat. Biotechnol.* **2011**, *29*, 693.
- [6] S. Galanie, K. Thodey, I. J. Trenchard, M. F. Terrante, C. D. Smolke, *Science* **2015**, *349*, 1095–1100.
- [7] D.-K. Ro, E. M. Paradise, M. Ouellet, K. J. Fisher, K. L. Newman, J. M. Ndungu, K. A. Ho, R. A. Eachus, T. S. Ham, J. Kirby, *Nature* **2006**, *440*, 940.
- [8] H. Fang, D. Li, J. Kang, P. Jiang, J. Sun, D. Zhang, *Nat. Commun.* **2018**, *9*, 4917.
- [9] T. M. Hsu, D. H. Welner, Z. N. Russ, B. Cervantes, R. L. Prathuri, P. D. Adams, J. E. Dueber, *Nat. Chem. Biol.* **2018**, *14*, 256.
- [10] S. Elleuche, C. Schäfers, S. Blank, C. Schröder, G. Antranikian, *Curr. Opin. Microbiol.* **2015**, *25*, 113–119.
- [11] P. Turner, G. Mamo, E. N. Karlsson, *Microb. Cell Fact.* **2007**, *6*, 9.
- [12] a) J. A. Coker, *F1000Res.* **2016**, *5*, 396; b) Y. Gumulya, N. J. Boxall, H. N. Khaleque, V. Santala, R. P. Carlson, A. H. Kaksonen, *Gene* **2018**, *9*, 116.
- [13] a) P. Q. Nguyen, Z. Botyanszki, P. K. R. Tay, N. S. Joshi, *Nat. Commun.* **2014**, *5*, 4945; b) P. Q. Nguyen, N. M. D. Courchesne, A. Duraj-Thatte, P. Praveschotinunt, N. S. Joshi, *Adv. Mater.* **2018**, *30*, 1704847; c) A. Y. Chen, C. Zhong, T. K. Lu, *ACS Synth Biol.* **2015**, *4*, 8–11.
- [14] X. Tong, T. T. Barberi, C. H. Botting, S. V. Sharma, M. J. Simmons, T. W. Overton, R. J. Goss, *Microb. Cell Fact.* **2016**, *15*, 180.
- [15] a) H.-C. Flemming, J. Wingender, *Nat. Rev. Microbiol.* **2010**, *8*, 623; b) H. Boudarel, J.-D. Mathias, B. Blaysat, M. Grédiac, *NPJ Biofilms Microbiomes* **2018**, *4*, 17.
- [16] N. Qureshi, B. A. Annous, T. C. Ezeji, P. Karcher, I. S. Maddox, *Microb. Cell Fact.* **2005**, *4*, 24.

- [17] D. C. Volke, P. I. Nickel, *Adv. Biosystems* **2018**, *2*, 1800111.
- [18] P. Larsen, J. L. Nielsen, D. Otzen, P. H. Nielsen, *Appl. Environ. Microbiol.* **2008**, *74*, 1517–1526.
- [19] a) M. M. Barnhart, M. R. Chapman, *Annu. Rev. Microbiol.* **2006**, *60*, 131–147; b) T. R. Costa, C. Felisberto-Rodrigues, A. Meir, M. S. Prevost, A. Redzej, M. Trokter, G. Waksman, *Nat. Rev. Microbiol.* **2015**, *13*, 343.
- [20] M. G. Nussbaumer, P. Q. Nguyen, P. K. Tay, A. Naydich, E. Hysi, Z. Botyanski, N. S. Joshi, *ChemCatChem* **2017**, *9*, 4328–4333.
- [21] a) E. Kalyoncu, R. E. Ahan, T. T. Olmez, U. O. S. Seker, *RSC Adv.* **2017**, *7*, 32543–32551; b) U. O. S. Seker, A. Y. Chen, R. J. Citorik, T. K. Lu, *ACS Synth. Biol.* **2017**, *6*, 266–275.
- [22] T. Onur, E. Yuca, T. T. Olmez, U. O. S. Seker, *J. Colloid Interface Sci.* **2018**, *520*, 145–154.
- [23] C. Zhong, T. Gurry, A. A. Cheng, J. Downey, Z. Deng, C. M. Stultz, T. K. Lu, *Nat. Nanotechnol.* **2014**, *9*, 858.
- [24] a) E. P. DeBenedictis, J. Liu, S. Keten, *Sci. Adv.* **2016**, *2*, e1600998; b) Y. Z. Zhou, D. Smith, B. J. Leong, K. Brannstrom, F. Almqvist, M. R. Chapman, *J. Biol. Chem.* **2012**, *287*, 35092–35103.
- [25] A. Y. Chen, Z. Deng, A. N. Billings, U. O. Seker, M. Y. Lu, R. J. Citorik, B. Zakeri, T. K. Lu, *Nat. Mater.* **2014**, *13*, 515.
- [26] a) Y. Cao, Y. Feng, M. D. Ryser, K. Zhu, G. Herschlag, C. Cao, K. Marusak, S. Zauscher, L. You, *Nat. Biotechnol.* **2017**, *35*, 1087–1093; b) D. T. Schmieden, S. J. Basalo Vázquez, H. C. Sangüesa, M. van der Does, T. Idema, A. S. Meyer, *ACS Synth. Biol.* **2018**, *7*, 1328–1337.
- [27] a) C. Y. Hu, M. K. Takahashi, Y. Zhang, J. B. Lucks, *ACS Synth. Biol.* **2018**, *7*, 1507–1518; b) A. A. Green, J. M. Kim, D. Ma, P. A. S. Ilver, J. J. Collins, P. Yin, *Nature* **2017**, *548*, 117–121.
- [28] A. A. Green, P. A. Silver, J. J. Collins, P. Yin, *Cell* **2014**, *159*, 925–939.
- [29] K. Pardee, A. A. Green, M. K. Takahashi, D. Braff, G. Lambert, J. W. Lee, T. Ferrante, D. Ma, N. Donghia, M. Fan, N. M. Daringer, I. Bosch, D. M. Dudley, D. H. O'Connor, L. Gehrke, J. J. Collins, *Cell* **2016**, *165*, 1255–1266.
- [30] M. K. Takahashi, X. Tan, A. J. Dy, D. Braff, R. T. Akana, Y. Furuta, N. Donghia, A. Ananthakrishnan, J. J. Collins, *Nat. Commun.* **2018**, *9*, 3347.
- [31] P. Siuti, J. Yazbek, T. K. Lu, *Nat. Biotechnol.* **2013**, *31*, 448–452.
- [32] a) A. Courbet, D. Endy, E. Renard, F. Molina, J. Bonnet, *Sci. Transl. Med.* **2015**, *7*, 289ra83; b) M. Müller, S. Auslander, A. Spinnler, D. Auslander, J. Sikorski, M. Folcher, M. Fussenegger, *Nat. Chem. Biol.* **2017**, *13*, 309–316.
- [33] N. Roquet, A. P. Soleimany, A. C. Ferris, S. Aaronson, T. K. Lu, *Science* **2016**, *353*, 6297.
- [34] C. A. Merrick, J. Zhao, S. J. Rosser, *ACS Synth. Biol.* **2018**, *7*, 299–310.
- [35] Y. J. Oh, Y. Cui, H. Kim, Y. Li, P. Hinterdorfer, S. Park, *Biophys. J.* **2013**, *104*, 513a.
- [36] a) C. Fux, J. W. Costerton, P. S. Stewart, P. Stoodley, *Trends Microbiol.* **2005**, *13*, 34–40; b) C. L. Abberton, L. Bereschenko, P. W. van der Wiele, C. J. Smith, *Appl. Environ. Microbiol.* **2016**, AEM, 01569-01516; c) J. R. Sheldon, M.-S. Yim, J. H. Saliba, W.-H. Chung, K.-Y. Wong, K. T. Leung, *Appl. Environ. Microbiol.* **2012**, *78*, 8331–8339; d) A. Bridier, R. Briandet, V. Thomas, F. Dubois-Brissonnet, *Biofouling* **2011**, *27*, 1017–1032; e) T. Juhna, D. Birzniece, J. Rubulis, *Appl. Environ. Microbiol.* **2007**, *73*, 3755–3758.
- [37] a) A. Ito, A. Taniuchi, T. May, K. Kawata, S. Okabe, *Appl. Environ. Microbiol.* **2009**, *75*, 4093–4100; b) P. S. Stewart, *Int. J. Med. Microbiol.* **2002**, *292*, 107.
- [38] a) M. R. Hammar, A. Arnqvist, Z. Bian, A. Olsén, S. Normark, *Mol. Microbiol.* **1995**, *18*, 661–670; b) F. Mergulhão, D. K. Summers, G. A. Monteiro, *Biotechnol. Adv.* **2005**, *23*, 177–202.
- [39] a) Y. Zhou, D. R. Smith, D. A. Hufnagel, M. R. Chapman in *Bacterial Cell Surfaces: Methods and Protocols* (A. H. Delacour), Springer, New York, **2013**, pp. 53–75; b) M. L. Evans, M. R. Chapman, *Biochim. Biophys. Acta Mol. Cell Res.* **2014**, *1843*, 1551–1558.
- [40] K. D. Piatkevich, J. Hult, O. M. Subach, B. Wu, A. Abdulla, J. E. Segall, V. V. Verkhusha, *Proc. Natl. Acad. Sci. USA* **2010**, *107*, 5369–5374.
- [41] J. Bonnet, P. Yin, M. E. Ortiz, P. Subsoontorn, D. Endy, *Science* **2013**, *340*, 599–603.

Manuscript received: December 4, 2018

Revised manuscript received: March 8, 2019

Accepted manuscript online: March 8, 2019

Version of record online: May 15, 2019